Pairing in Few-Fermion Systems with Attractive Interactions

G. Zürn,[1,2,*] A. N. Wenz,[1,2] S. Murmann,[1,2] A. Bergschneider,[1,2] T. Lompe,[1,2,3] and S. Jochim[1,2,3]

[1]*Physikalisches Institut, Ruprecht-Karls-Universität Heidelberg, 69120 Heidelberg, Germany*

[2]*Max-Planck-Institut für Kernphysik, Saupfercheckweg 1, 69117 Heidelberg, Germany*

[3]*ExtreMe Matter Institute EMMI, GSI Helmholtzzentrum für Schwerionenforschung, 64291 Darmstadt, Germany*

(Received 18 July 2013; published 22 October 2013)

We study quasi-one-dimensional few-particle systems consisting of one to six ultracold fermionic atoms in two different spin states with attractive interactions. We probe the system by deforming the trapping potential and by observing the tunneling of particles out of the trap. For even particle numbers, we observe a tunneling behavior that deviates from uncorrelated single-particle tunneling indicating the existence of pair correlations in the system. From the tunneling time scales, we infer the differences in interaction energies of systems with different number of particles, which show a strong odd-even effect, similar to the one observed for neutron separation experiments in nuclei.

DOI: 10.1103/PhysRevLett.111.175302 PACS numbers: 67.85.Lm

Pairing between distinguishable fermions with an attractive interparticle interaction leads to fascinating phenomena in a variety of vastly different systems. In metals at sufficiently low temperature, pairs of electrons can form a superfluid, as described by Bardeen, Cooper, and Schrieffer in their BCS theory of superconductivity [1]. With the use of dilute gases of ultracold atoms, where the interparticle interactions can be tuned freely using Feshbach resonances [2], it was shown that such BCS pairs can be smoothly converted into bosonic molecules [3], which leads to a continuous crossover from a BCS-like superfluid to a BEC of molecules [4–7]. In finite Fermi systems, pairing has been studied extensively in the context of nuclear physics [8–10]. Here, the pairing caused by the attractive interaction between the nucleons leads to an enhanced stability of systems with an even number of neutrons or protons [10]. For systems with fully closed shells—the so-called magic nuclei—stability is further enhanced.

Recently, it has become possible to prepare finite systems of ultracold fermions in well-defined quantum states [11]. In such a system, one has direct experimental control over key parameters such as the particle number and the depth and shape of the confining potential. Combined with the ability to tune the interparticle interactions [2,12], this makes this system uniquely suited to study pairing in a controlled environment.

In this work, we study how pairing affects few-particle systems consisting of one to six ultracold atoms in two different spin states, labeled $|\uparrow\rangle$ and $|\downarrow\rangle$, confined in a cigar-shaped optical microtrap [13]. We deterministically prepare these systems in their ground state using the preparation scheme developed in Ref. [11]. Our microtrap has typical trap frequencies of $\omega_{\parallel} = 2\pi \times 1.488(14)$ kHz [14] in longitudinal and $\omega_{\perp} = 2\pi \times 14.22(35)$ kHz [15] in perpendicular directions. In addition to the optical potential, we can apply a linear potential in longitudinal direction by applying a magnetic field gradient. A full description of the potential shape as determined in Ref. [14] is given in Ref. [16].

As in our few-fermion systems, all energy scales are much smaller than $\hbar\omega_{\perp}$, the system can be treated as quasi-one-dimensional [17]. In this one-dimensional (1D) environment, the interaction between distinguishable particles can be described by a contact interaction whose coupling constant $g_{1\downarrow}$ can be tuned by a confinement-induced resonance [18] [see Fig. 1(b)].

In a first set of experiments we study the emergence of pair correlations in a two-particle system. Therefore, we prepare two particles, one in state $|\uparrow\rangle$ and one in state $|\downarrow\rangle$, in the ground state of the trapping potential. To probe the system, we employ the same method as described in Ref. [14]: We lower the depth of the optical potential such that there is a potential barrier of well-defined height through which the particles can tunnel out of the trap. After a certain hold time, we ramp the potential back up and measure the number of particles remaining in the trap. By performing many of these measurements at different hold times, we measure the time evolution of the probabilities $P_2(t)$, $P_1(t)$, and $P_0(t)$ to find two, one, or zero particles in the tilted potential. From these probabilities we get the mean particle number $\bar{N}(t) = 2P_2(t) + 1P_1(t)$ whose time evolution is shown in Fig. 1(a) for three different values of the interparticle interaction.

For a system of two noninteracting particles, the loss follows an exponential decay with a tunneling rate $\gamma_{s_0} \approx 30\,\mathrm{s}^{-1}$. In the presence of an attractive interparticle interaction (i.e., $g_{1\downarrow} < 0$), the energy of the system is reduced. This leads to an effective increase in the height of the tunneling barrier, and therefore the tunneling slows down. Consequently, the tunneling of the particles is no longer independent and thus cannot be described by a simple exponential decay.

To describe the correlated tunneling of the two particles, we use a simple model that takes into account two different

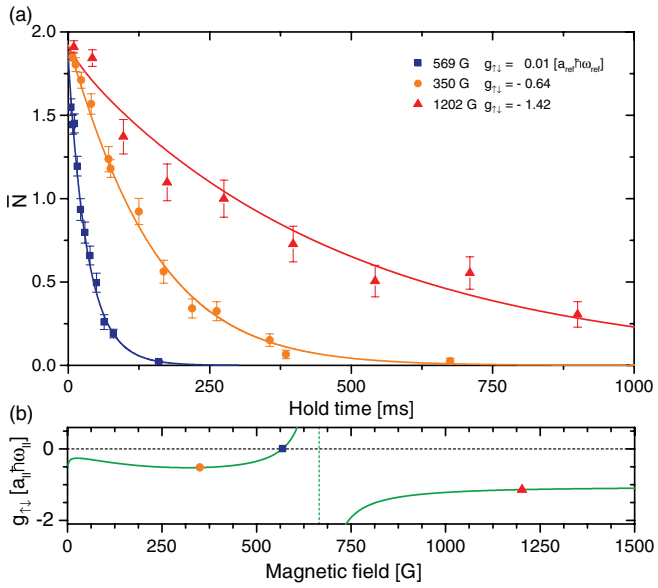

FIG. 1 (color online). (a) To study a system of two attractively interacting fermions, we study its tunneling dynamics by creating a barrier of fixed height and recording the number of particles remaining in the trap after different hold times. We find that the tunneling slows down as we increase the strength of the interparticle interaction from zero (blue squares) to intermediate (orange dots) or to larger values (red triangles), where the solid lines are fits according to the tunneling model described in the text and the errors are the standard error of the mean of 100 individual measurements. This shows the increase of the effective barrier height due to the energy shift caused by the attractive interaction. (b) Coupling constant $g_{\uparrow\downarrow}$ in the untilted potential as a function of the magnetic field with $a_{\parallel} = \sqrt{\hbar/\mu\omega_{\parallel}}$. Note that $g_{\uparrow\downarrow}$ depends on the parameters of the deformed potential and is therefore given in units of $a_{\mathrm{ref}}\hbar\omega_{\mathrm{ref}}$ for the different measurements [16].

loss processes (see inset in Fig. 2). The first is pair tunneling, which we define as two particles leaving the trap at the same time. The rate at which this process occurs is labeled γ_p. The second process is subsequent single-particle tunneling. Here, one particle tunnels first, while the other particle remains in the unperturbed ground state of the trap. In this case, the first particle tunnels with a rate $2\gamma_s$, which is determined by the effective height of the tunneling barrier which in turn depends on the interaction energy of the two particles. For the second particle, there is no interaction shift, and consequently it leaves the trap with the rate γ_{s_0} measured for the noninteracting system.

To relate these rates to our measured probabilities $P_i(t)$, we set up a set of rate equations that give the probabilities to find two, one, or zero particles in the trap as a function of the hold time. The probability $P_2(t)$ to find two particles in the trap decreases with the sum of the single-particle tunneling rate $2\gamma_s$ and the pair tunneling rate γ_p

$$\frac{dP_2(t)}{dt} = -(2\gamma_s + \gamma_p)P_2(t). \tag{1}$$

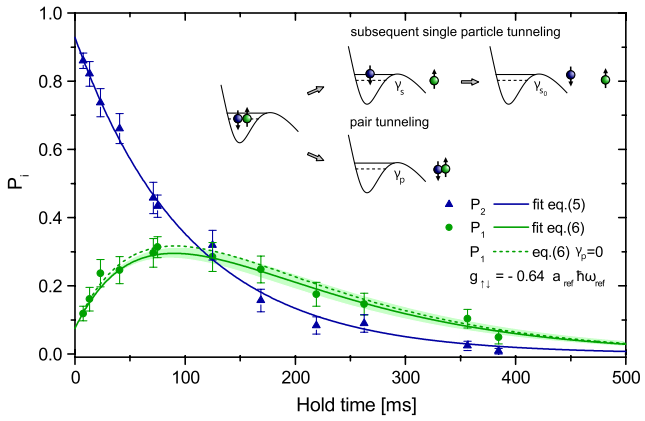

FIG. 2 (color online). Measured time evolution of the probabilities $P_1(t)$ and $P_2(t)$ to find one (green dots) or two (blue triangles) particles in the tilted potential at an intermediate interaction strength of $g_{\uparrow\downarrow} = -0.64$. The blue solid line shows a fit of Eq. (5) to $P_2(t)$ with free parameters f and γ_2. The green line shows the fit to $P_1(t)$ with the single free parameter γ_p, where the shaded region indicates the uncertainty that results from our determination of the shape of the trapping potential. For comparison, the dashed line shows the result from Eq. (6) with γ_p set to 0, which is also consistent with our data. The errors are the 68% confidence interval of about 100 individual measurements. The inset shows a sketch of the loss processes included in our tunneling model: subsequent single-particle tunneling with rates γ_s and γ_{s_0} and direct pair tunneling with a rate γ_p.

This rate equation can be easily solved, and the decay law for the two-particle probability reads

$$P_2(t) = e^{-(2\gamma_s+\gamma_p)t}. \tag{2}$$

The rate equation for the probability $P_1(t)$ is given by

$$\frac{dP_1(t)}{dt} = 2\gamma_s P_2(t) - \gamma_{s_0} P_1(t), \tag{3}$$

where two-particle systems become one-particle systems with the rate $2\gamma_s$, where γ_s is the rate with which one of the particles leaves the trap. These systems then decay into zero-particle systems with the rate γ_{s_0}. Assuming a perfect preparation fidelity for the initial sample, the initial conditions for this equation are $P_2(0) = 1$ and $P_1(0) = P_0(0) = 0$ and one obtains a probability

$$P_1(t) = \frac{2\gamma_s}{2\gamma_s + \gamma_p - \gamma_{s_0}}[e^{-\gamma_{s_0}t} - e^{-(2\gamma_s+\gamma_p)t}] \tag{4}$$

to find a single particle in the trap.

To describe our experiments, we have to take into account two additional effects. The first is the finite preparation fidelity $0 \le f \le 1$, which defines the starting conditions of the decay. The second is that changing the magnetic offset field to tune the interaction strength affects the magnetic moment of the atoms. This leads to a state-dependent change in the shape of the tilted potential

as a function of the magnetic field [16]. Consequently, the tunneling rates also obtain a spin dependence that leads to the modified solutions

$$P_2(t) = f e^{-(\gamma_{s|\downarrow\rangle}+\gamma_{s|\uparrow\rangle}+\gamma_p)t} = f e^{-\gamma_2 t} \tag{5}$$

and

$$\begin{aligned} P_1(t) = f\Big(&\frac{\gamma_{s|\uparrow\rangle}}{\gamma_2 - \gamma_{s_0|\downarrow\rangle}}[e^{-\gamma_{s_0|\downarrow\rangle}t} - e^{-\gamma_2 t}] \\ &+ \frac{\gamma_{s|\downarrow\rangle}}{\gamma_2 - \gamma_{s_0|\uparrow\rangle}}[e^{-\gamma_{s_0|\uparrow\rangle}t} - e^{-\gamma_2 t}]\Big) \\ &+ (1-f)\Big(\frac{1}{2}e^{-\gamma_{s_0|\uparrow\rangle}t} + \frac{1}{2}e^{-\gamma_{s_0|\downarrow\rangle}t}\Big) \end{aligned} \tag{6}$$

with the spin-dependent rate constants $\gamma_{s|\uparrow\rangle}$, $\gamma_{s|\downarrow\rangle}$, $\gamma_{s_0|\uparrow\rangle}$, and $\gamma_{s_0|\downarrow\rangle}$. In Eq. (6) the first (second) term corresponds to a former two-particle system where the $|\uparrow\rangle$ ($|\downarrow\rangle$) particle has tunneled first whereas the last term accounts for the single-particle systems that are present due to the finite preparation fidelity.

To determine the rates for single-particle and pair tunneling, we first fit our data for $P_2(t)$ with Eq. (5) and extract the combined loss rate γ_2 and the preparation fidelity. As fitting all remaining parameters to our data for $P_1(t)$ would be unstable, we independently determine $\gamma_{s_0|\uparrow\rangle}$ and $\gamma_{s_0|\downarrow\rangle}$ in a series of separate experiments with single $|\uparrow\rangle$ or $|\downarrow\rangle$ particles [16]. To further reduce the number of fit parameters, we make use of the fact that $\gamma_{s|\uparrow\rangle}$ and $\gamma_{s|\downarrow\rangle}$ are linked by the shape of the potential that we can infer from our measurements of $\gamma_{s_0|\uparrow\rangle}$ and $\gamma_{s_0|\downarrow\rangle}$. As we already know, $\gamma_2 = \gamma_{s|\uparrow\rangle} + \gamma_{s|\downarrow\rangle} + \gamma_p$; this leaves only one free parameter for our fit: the pair tunneling rate γ_p. Details on the fitting procedure can be found in Ref. [16]. As an example, the measured values for $P_2(t)$, $P_1(t)$, and the resulting fits for an interaction strength of $g_{\uparrow\downarrow} = -0.64$ are shown in Fig. 2 [19].

For $g_{\uparrow\downarrow} > -0.59$, we observe no pair tunneling. For $g_{\uparrow\downarrow} = -0.64$, we find a pair tunneling rate of $\gamma_p/\gamma_2 = 7(4)(10) \times$ (stat)(syst)%. Therefore, our data are consistent with a model which only considers subsequent single-particle tunneling. For stronger interaction, pair tunneling is expected to play a stronger role. However, in our measurements for $g_{\uparrow\downarrow} < -0.64$, the probability of finding a single particle in the trap is only a few percent, which is as small as the errors, and consequently we cannot resolve to which extent the two particles tunnel as a bound object.

To compare the tunneling dynamics at different interaction strengths that occur on time scales differing by almost 2 orders of magnitude, we rescale the data onto a common axis by plotting $P_1(t)$ as a function of the mean particle number (see Fig. 3 left panel).

For a noninteracting system (blue), we find that the probability of finding one atom follows that of completely uncorrelated tunneling indicated by the black dashed parabola $P_1 = \bar{N} - \bar{N}^2/2$. For increasing attractive

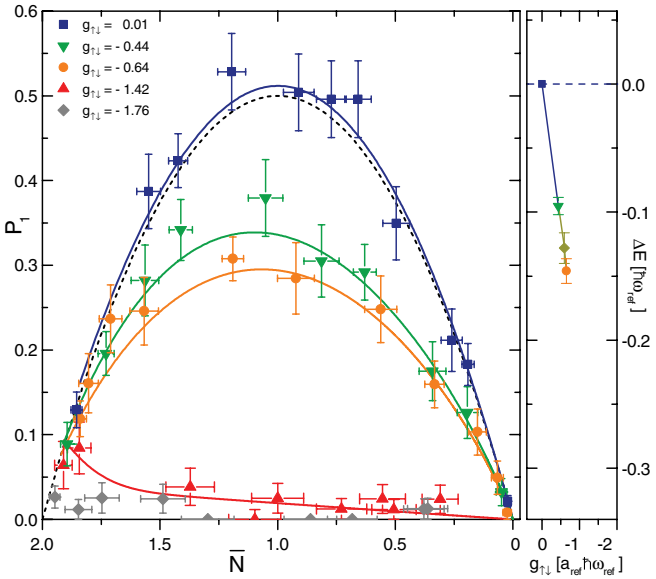

FIG. 3 (color online). Probability of finding a single particle in the trap plotted as a function of the mean particle number $\bar{N}$. The solid lines show the results of fits to the data according to our tunneling model (see Fig. 2). For a noninteracting system, the probability follows the expectation value of completely uncorrelated tunneling given by the black dashed line. For increasing interaction strengths, it becomes less likely to find a single particle in the trap, which we interpret as a result of increased pair correlations. To quantify this effect, we plot the interaction energy up to intermediate interaction strength as a function of $g_{\uparrow\downarrow}$ in the right panel. Here, pair tunneling is not considered in the analysis as it does not seem to play an important role at these interaction strengths.

interaction, the tunneling of the two particles is not uncorrelated anymore and we observe that the probability of finding a single particle in the trap decreases dramatically. This decrease in $P_1(t)$ can be explained by the fact that for larger interaction strengths the two-particle system experiences a larger effective barrier height and the tunneling rate γ_s of the first particle decreases, whereas the tunneling rate γ_{s_0} of the remaining particle is not affected. This leads to a decrease of the ratio γ_s/γ_{s_0} and therefore a lower probability to observe a single particle in the trap, which is well described by our tunneling model.

In the regime of weak interactions ($g > -0.64$) where pair tunneling plays only a negligible role, we use our model to determine the amount of interaction energy that is released as the first particle tunnels from the trap, which we call the separation energy. This is done in an iterative process where we vary E_{int} and calculate $\gamma_{s|\uparrow\rangle}$ and $\gamma_{s|\downarrow\rangle}$ using a WKB calculation until the tunneling rates match the ones determined by a least-squares fit to the P_1 data (Supplemental Material [16]). One should note that our approach does not take into account the wave function overlap of the trapped state and the continuum state within the tunneling barrier. This leads to a systematic error in the interaction energy comparable to the one observed for

repulsively interacting systems [14,20], which has recently been addressed in Ref. [21]. However, the qualitative behavior of the separation energy at fixed particle number or at fixed interaction strength is not expected to be altered by this systematic effect.

For a two-particle system, the separation energy corresponds to the full interaction energy of the system. We clearly observe an increase of this interaction energy as a function of coupling strength, which is plotted in the right panel of Fig. 3. Since in a 1D system a decrease of the energy of the two-particle ground state leads to a collapse of the two-particle wave function, this corresponds to an increase of the local pair correlation $g^{(2)}(0)$ [22,23]. This energy measurement therefore directly shows the appearance of pairing in our attractively interacting two-particle system.

After having used the two-particle system to understand the tunneling dynamics and establishing a method to determine the separation energies of our system, we can now study how the observed pairing affects larger systems. In nuclear physics such pairing is one of the key ingredients required to obtain a quantitative understanding of the stability and binding energies of nuclei. One of its most pronounced consequences is the odd-even effect: systems with an even number of neutrons or protons have larger binding energies and increased stability against decay. To study this phenomenon in our model system, we measure the separation energy for two- to six-particle systems with an interaction strength of $g_{\uparrow\downarrow} \approx -0.6$ (Supplemental Material [16]) and observe a clearly enhanced stability of systems with even particle number (see Fig. 4).

In addition to this odd-even effect, we also observe a general decrease of the separation energy with growing particle number. To quantify this effect, we consider the single-particle levels in the trap as the shells of our 1D system and use the difference in the separation energy between open- and closed-shell systems to estimate the contributions of intra- and intershell pairing. For the two-particle system, the separation energy ΔE directly corresponds to the pairing energy E_{00} of the two particles on the lowest shell. For $N = 3$, the third particle has no interaction partner on its own shell. However, its separation energy is still strongly reduced compared to that of the noninteracting case. This suggests a strong intershell pairing (E_{10}) to the particles on the shell below. For $N = 4$, the separation energy is then given by the sum of the intershell interaction energy E_{10} and the intrashell interaction energy E_{11}, which are of similar size.

To understand the observed scaling of the separation energy with particle number, we first consider a weakly interacting system. In this case, two particles on the same shell obtain an interaction shift proportional to the coupling constant, as they have the same spatial wave function. To first order, particles on closed shells have the same wave function, and therefore Pauli blocking prevents all other

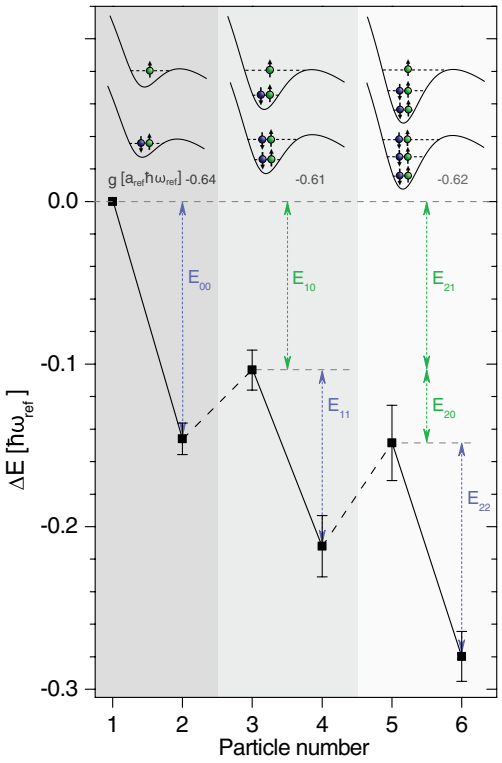

FIG. 4 (color online). Separation energies for systems of $N = 1, \ldots, 6$ particles at an interaction strength of $g_{\uparrow\downarrow} \approx -0.6$. The small difference in $g_{\uparrow\downarrow}$ for the different particle numbers is due to the dependence of the coupling strength on the depth of the optical potential. The separation energies are normalized by the level spacing of the two uppermost trap states. The error bars show the relative uncertainty originating from the statistical errors of the fits of γ_N and $\gamma_{s_0|\uparrow\rangle}$. The arrows indicate the contributions E_{ii} and E_{ij} of the intrashell (blue) and intershell (green) interaction to the separation energy.

particles on different shells from having any overlap with them. Only in a second-order process where the wave functions of the particles in the closed shell are modified due to the interactions with a particle on a different shell does the overlap become nonzero. From the fact that the observed intershell pairing energy is comparable to the intrashell pairing energy, we conclude that the different shells have a significant overlap and our system is no longer in the weakly interacting regime. Therefore, our results can serve as a test for theories that predict the disappearance of shell structures in strongly interacting few-body systems [24,25].

In conclusion, we have used tunneling experiments to study quasi-1D few-fermion systems with attractive interactions and observed the emergence of correlations in the tunneling dynamics. We have developed a model that accurately describes the tunneling dynamics of the two-particle system and used it to infer the presence of pair correlations. We have then used this model to determine the separation energies for larger systems and identified the contributions of intra- and intershell pairing to the

observed odd-even effect. These measurements open the door to study how the shell structure of a finite system evolves in the BEC-BCS crossover [24,25]. This would also be the first step towards studying the emergence of BCS-like superfluidity in a finite system of ultracold atoms through studies of rotational excitations [8,26].

We thank Massimo Rontani for inspiring discussions and valuable theoretical input. We thank Shannon Withlock for helpful discussions. The authors gratefully acknowledge support from ERC starting Grant No. 279697, the Helmholtz Alliance HA216/EMMI, and the Heidelberg Center for Quantum Dynamics. G. Z. and A. N. W. acknowledge support from the IMPRS-QD.

*gerhard.zuern@physi.uni-heidelberg.de

[1] J. Bardeen, L. N. Cooper, and J. R. Schrieffer, Phys. Rev. **108**, 1175 (1957).
[2] C. Chin, R. Grimm, P. Julienne, and E. Tiesinga, Rev. Mod. Phys. **82**, 1225 (2010).
[3] C. A. Regal, C. Ticknor, J. L. Bohn, and D. S. Jin, Nature (London) **424**, 47 (2003).
[4] A. J. Leggett, J. Phys. (Paris), Colloq. **41**, C7-19 (1980).
[5] P. Nozières and S. S. Rink, J. Low Temp. Phys. **59**, 195 (1985).
[6] M. Bartenstein, A. Altmeyer, S. Riedl, S. Jochim, C. Chin, J. H. Denschlag, and R. Grimm, Phys. Rev. Lett. **92**, 120401 (2004).
[7] M. W. Zwierlein, J. R. A. Shaeer, A. Schirotzek, C. H. Schunck, and W. Ketterle, Nature (London) **435**, 1047 (2005).
[8] A. Migdal, Nucl. Phys. **13**, 655 (1959).
[9] V. Zelevinsky and A. Volya, Phys. At. Nucl. **66**, 1781 (2003).
[10] D. Brink and R. Broglia, *Nuclear Superfluidity: Pairing in Finite Systems* (Cambridge University Press, Cambridge, England, 2005).
[11] F. Serwane, G. Zürn, T. Lompe, T. B. Ottenstein, A. N. Wenz, and S. Jochim, Science **332**, 336 (2011).
[12] G. Zürn, T. Lompe, A. N. Wenz, S. Jochim, P. S. Julienne, and J. M. Hutson, Phys. Rev. Lett. **110**, 135301 (2013).
[13] In this work, the two spin states $|{\downarrow}\rangle$ and $|{\uparrow}\rangle$ are realized by the $F = 1/2$, $m_F = 1/2$ and $F = 3/2$, $m_F = -3/2$ hyperfine states of ^{6}Li.
[14] G. Zürn, F. Serwane, T. Lompe, A. N. Wenz, M. G. Ries, J. E. Bohn, and S. Jochim, Phys. Rev. Lett. **108**, 075303 (2012).
[15] S. Sala, G. Zürn, T. Lompe, A. N. Wenz, S. Murmann, F. Serwane, S. Jochim, and A. Saenz, Phys. Rev. Lett. **110**, 203202 (2013).
[16] See the Supplemental Material at http://link.aps.org/supplemental/10.1103/PhysRevLett.111.175302 for details on the determination of the state-dependent potential and for the fitting procedure.
[17] Z. Idziaszek and T. Calarco, Phys. Rev. A **71**, 050701 (2005).
[18] M. Olshanii, Phys. Rev. Lett. **81**, 938 (1998).
[19] In the deformed potential $g_{\uparrow\downarrow}$ is given in units of $a_{\mathrm{ref}}\hbar\omega_{\mathrm{ref}}$ [16].
[20] M. Rontani, Phys. Rev. Lett. **108**, 115302 (2012).
[21] M. Rontani, arXiv:1308.2174 [Phys. Rev. A (to be published)].
[22] T. Busch, B.-G. Englert, K. Rzazewski, and M. Wilkens, Found. Phys. **28**, 549 (1998).
[23] S. Franke-Arnold, S. Barnett, G. Huyet, and C. Sailliot, Eur. Phys. J. D **22**, 373 (2003).
[24] M. Rontani, J. R. Armstrong, Y. Yu, S. Aberg, and S. M. Reimann, Phys. Rev. Lett. **102**, 060401 (2009).
[25] N. T. Zinner, K. Mølmer, C. Özen, D. J. Dean, and K. Langanke, Phys. Rev. A **80**, 013613 (2009).
[26] S. Grebenev, J. P. Toennies, and A. F. Vilesov, Science **279**, 2083 (1998).